JACS
JOURNAL OF THE AMERICAN CHEMICAL SOCIETY

Subscriber access provided by American Chemical Society

Article

Synergy of Intramolecular Hydrogen-Bonding Network in *myo*-Inositol 2-Monophosphate: Theoretical Investigations into the Electronic Structure, Proton Transfer, and p*K*

Ping Yang, Pushpalatha P. N. Murthy, and Richard E. Brown

J. Am. Chem. Soc., **2005**, 127 (45), 15848-15861• DOI: 10.1021/ja053371u • Publication Date (Web): 20 October 2005

Downloaded from http://pubs.acs.org on March 25, 2009

More About This Article

Additional resources and features associated with this article are available within the HTML version:

- Supporting Information
- Links to the 2 articles that cite this article, as of the time of this article download
- Access to high resolution figures
- Links to articles and content related to this article
- Copyright permission to reproduce figures and/or text from this article

View the Full Text HTML

ACS Publications
High quality. High impact.

Journal of the American Chemical Society is published by the American Chemical Society. 1155 Sixteenth Street N.W., Washington, DC 20036

J|A|C|S
ARTICLES
Published on Web 10/20/2005

Synergy of Intramolecular Hydrogen-Bonding Network in *myo*-Inositol 2-Monophosphate: Theoretical Investigations into the Electronic Structure, Proton Transfer, and pK_a

Ping Yang, Pushpalatha P. N. Murthy, and Richard E. Brown*

Contribution from the Department of Chemistry, Michigan Technological University, Houghton, Michigan 49931

Received May 24, 2005; E-mail: rebrown@mtu.edu

Abstract: This work demonstrates the pivotal role that an intramolecular hydrogen-bonding network (intra-HBN) plays in the determination of the conformation of *myo*-inositol 2-monophosphate (Ins(2)P_1), a member of the inositol phosphate family of compounds, which are important participants in the role that phosphates play in biological and environmental chemistry. For biologically significant compounds that contain phosphate and hydroxyl groups, Ins(2)P_1 is a model system for studying both the primary forces that determine their conformations and their chemical properties from the effect of phosphate group addition. We performed ab initio calculations to determine the intra-HBN within important thermally accessible conformations for neutral Ins(2)P_1 and its anions, Ins(2)P_1^{1-} and Ins(2)P_1^{2-}. The results show that the global minima prefer 1a/5e structures where the phosphate group is in the axial position with all −OH groups in the equatorial positions. The calculations of transition state structures for ring inversion at each ionization state predict an activation energy of 18.16 kcal/mol for the neutral species in water, while the activation energy is lower for the charged compounds, 15.62 kcal/mol for Ins(2)P_1^{1-} and 12.48 kcal/mol for Ins(2)P_1^{2-}. The pK_a values of Ins(2)P_1 were calculated by modeling the solvent as a polarizable continuum medium (PCM) and as explicit solvent molecules. These values are in good agreement with experimental data. A novel four-center pattern of hydrogen bonding was found to stabilize the system. The intramolecular proton transfer across a low barrier hydrogen bond between the charged phosphate and hydroxyl groups was found to occur under standard conditions with an activation energy that is less than 0.5 kcal/mol.

Introduction

The discovery that inositol phosphates play critical roles in various cellular processes including signal transduction, calcium regulation, and membrane biogenesis has triggered widespread interest in the structure, metabolism, and biological roles of inositol phosphates.[1−5] Inositol phosphates are composed of a cyclohexane ring with either a hydroxyl (−OH) or phosphate (−OPO(OH)$_2$) substituent on each carbon. Since each substituent can be placed in an equatorial (e) or axial (a) position, there are a large variety of stereochemical isomers (Figure 1).

Symmetric *myo*-inositol 2-monophosphate (Ins(2)P_1) is one of the important analogues involved in the study of the biological role of the inositol phosphate family of compounds, which are crucial participants in the role that phosphates play in biological and environmental chemistry (Figure 2).[6] Ins(2)P_1 is hydrolyzed by *myo*-inositol monophosphatase (IMP) in the metabolic pathway of inositol phosphates in living systems.[7] The conformation of Ins(2)P_1 is essential to understanding the mechanism of IMP which has been a subject of recent experimental research.[8−10] NMR investigations have shown that higher inositol phosphates can adopt either the 5a/1e or 1a/5e conformations which readily interconvert through ring inversion, the ease of which is dependent on the pH.[5,11−13] For example, *myo*-inositol hexakisdihydrogenphoshate, i.e., phytic acid, and some *myo*-inositol pentakisdihydrogenphosphates (such as Ins-

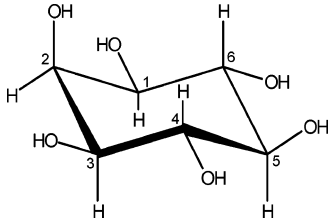

Figure 1. *myo*-Inositol.

(1) Toker, A. *Cell. Mol. Life Sci.* **2002**, *59*, 761−779.
(2) Irvine, R. F.; Schell, M. J. *Nat. Rev. Mol. Cell. Biol.* **2001**, *2*, 327−338.
(3) Vanhaesebroek, B.; Leevers, S.; Ahmadi, K.; Timms, J.; Katso, R.; Drisscoll, P. C.; Woscholski, R.; Parker, P. J.; Waterfield, M. D. *Annu. Rev. Biochem.* **2001**, *70*, 535−602.
(4) Shears, S. B. *Biochim. Biophys. Acta* **1998**, *1436*, 49−67.
(5) Loewus, F. A.; Murthy, P. P. N. *Plant Sci.* **2000**, *150*, 1−19.
(6) Fisher, S. K.; Novak, J. E.; Agranoff, B. W. *J. Neurochem.* **2002**, *82*, 736−754.
(7) Rio, E.; Shinomura, T.; Kaay, J.; Nichollas, D. G.; Downes, C. P. *J. Neurochem.* **1998**, *70*, 1662−1669.
(8) Fauroux, C. M.-J.; Lee, M.; Cullis, P. M.; Douglas, K. T.; Gore, M. G.; Freeman, S. *J. Med. Chem.* **2002**, *45*, 1363−1373.
(9) Nigou, J.; Dover, L. G.; Besra, G. S. *Biochemistry* **2002**, *41*, 4392−4398.
(10) Johnson, K. A.; Chen, L.; Yang, H.; Roberts, M. F.; Stec, B. *Biochemistry* **2001**, *40*, 618−630.
(11) Barrientos, L. G.; Murthy, P. P. N. *Carbohydr. Res.* **1996**, *296*, 36−54.
(12) Bauman, A. T.; Chateauneuf, G. M.; Brown, R. E.; Murthy, P. P. N. *Tetrahedron Lett.* **1999**, *40*, 4489−4492.
(13) Volkmann, C. J.; Chateauneuf, G. M.; Pradhan, J.; Bauman, A. T.; Brown, R. E.; Murthy, P. P. N. *Tetrahedron Lett.* **2002**, *43*, 4853−4856.

10.1021/ja053371u CCC: $30.25 **© 2005 American Chemical Society**

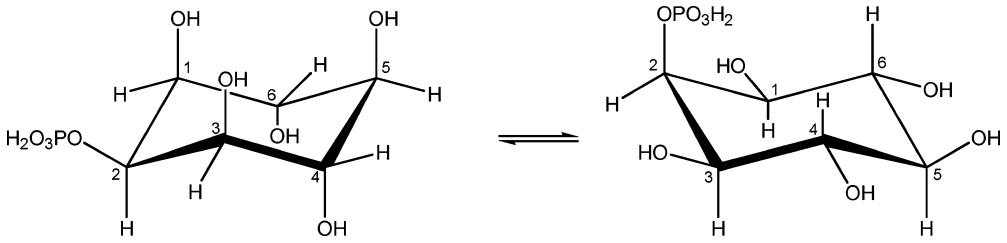

Figure 2. (a) 5a/1e conformation of Ins(2)P_1. (b) 1a/5e conformation of Ins(2)P_1.

(1,2,3,4,6)P_5 and Ins(,2,3,5,6)P_5) adopt the 1a/5e conformation in the pH range below 9.0 but the sterically hindered 5a/1e conformation above pH 9.5 (Figure 2). More importantly, inositol phosphates are models for compounds having both hydroxyl (−OH) and phosphate groups such as RNAs, nucleotides, and phosphorylated sugars. The intramolecular hydrogen-bonding interaction is critical to their biological functions. Results from these model systems will help to guide accurate simulations of proteins, RNAs, and membrane structures as well as provide information for the dynamical changes in response to post-translational phosphorylation. Although, in the past twenty years, *myo*-inositol phosphates have been investigated extensively by experimental methods and by some computational methods,[7,11,14−26] the intramolecular hydrogen bonding synergy in the determination of its conformations and properties has not gained enough attention. Direct experimental study of the effects of these hydrogen bonds is difficult. In this case, theoretical investigation is necessary.

Proton migration via a hydrogen bond has been identified as a fundamental mechanical process through which many chemical and biological functions are carried out. Especially in the field of biochemistry and molecular biology, proton transfer has come to be recognized as a significant component of enzyme catalysis and the transmission of ions through membranes. An intensive research effort has been applied to O−H···O$^-$ hydrogen bonds[24,27−29] in the absence of solvent effects. In this paper, a theoretical investigation to the intramolecular proton transfer across a hydrogen bond between the phosphate and hydroxyl groups is presented in both the gas and aqueous phases. A novel four-center pattern of hydrogen bonding was found with an unusual ability to stabilize the system in gas phase when proton transfer occurs.

It is generally understood that for substituents on the cyclohexane ring the more bulky substituents prefer the equatorial position in order to lower steric interactions. In the case of the Ins(2)P_1 molecule, a meso compound in which position 1 is equivalent to position 3 and position 4 is equivalent to position 6, there are two naturally occurring chair conformations. One chair conformation is with the phosphate group in the axial position and the five hydroxyl groups in equatorial position (5a/1e), and the other one is with the phosphate group is equatorial while the five hydroxyl groups are axial (1a/5e). Even though the hydroxyl group is a smaller substituent than the phosphate group, it is not clear if the sum of the steric effects of the five hydroxyl groups is larger than that of the phosphate group. Additionally, the repulsive steric interactions can be compensated by hydrogen bonding interactions. Since there is a total of seven hydroxyl groups in this molecule, intramolecular hydrogen bonding may certainly have a large cumulative effect on the preferred conformation. Thus it is not intuitively obvious which chair conformation will be the dominant one. Previous NMR data have shown that Ins(2)P_1 does not undergo chair−chair conversion (1a/5e ⇌ 5a/1e)[10] at room temperature and pressure while other *myo*-inositol phosphates which carry at least four vicinal equatorial phosphate groups readily undergo inversion at different pH.[30] To shed light on understanding the conformations of Ins(2)P_1 at different pH, calculations were completed on the conformations of neutral Ins(2)P_1^0 (at low pH), partially deprotonated Ins(2)P_1^{1-} (at intermediate pH), and fully deprotonated Ins(2)P_1^{2-} (at high pH). In this paper, we use ab initio methods and density functional theory to explore the global minimum energy conformations and the transition state structure for ring inversion of each species. These results will characterize the latent conformations, shapes, and stabilities of these inositol phosphates and thus help clarify the many biological functions that inositol phosphates and inositol lipids serve.

Besides the exploration of the electronic structure of the intramolecular hydrogen bonding network (intra-HBN), the pK_a of this phosphorylated compound was investigated as well. As proton transfer reactions are common in chemistry and biology,[31−33] it is important to quantify the tendency of the molecule to deprotonate its hydrogen atom as an acidic proton, i.e., the pK_a values. The evaluation of pK_a values is important for understanding the mechanisms of enzymes. They can be experimentally determined with some well-established meth-

(14) Berridge, M. J.; Downes, C. P.; Hanley, M. R. *Cell* **1989**, *59*, 411−419.
(15) Carlsson, N.-G.; Bergman, E.-L.; Skoglund, E.; Hasselblad, K.; Sandberg, A.-S. *J. Agric. Food Chem.* **2001**, *49*, 1695−1701.
(16) Greiner, R.; Alminger, M. L.; Carlsson, N.-G. *J. Agric. Food Chem.* **2001**, *49*, 2228−2233.
(17) Nigou, J.; Besra, G. S. *Biochem. J.* **2002**, *361*, 385−390.
(18) Pollack, S. J.; Attack, J. R.; Knowles, M. R.; McAlliste, G.; Ragan, C. I.; Baker, R.; Fletcher, S. R.; Iversen, L. L.; Broughton, H. B. *Proc. Natl. Acad. Sci. U.S.A.* **1994**, *91*, 5766−5770.
(19) Sculimbrene, B. R.; Morgan, A. J.; Miller, S. J. *J. Am. Chem. Soc.* **2002**, *124*, 11653−11656.
(20) Kuad, P.; Borkovec, M.; Murr, M. D. E.; Le Gall, T.; Mioskowski, C.; Spiess, B. *J. Am. Chem. Soc.* **2005**, *127*, 1323−1333.
(21) Riley, A. M.; Dozol, H.; Spiess, B.; Potter, B. V. L. *Biochem. Biophys. Res. Commun.* **2004**, *318*, 444−452.
(22) Dozol, H.; Maechling, C.; Graff, R.; Matsuda, A.; Shuto, S.; Spiess, B. *Biochim. Biophys. Acta* **2004**, *1671*, 1−8.
(23) Borkovec, M.; Spiess, B. *Phys. Chem. Chem. Phys.* **2004**, *6*, 1144−1151.
(24) Felemez, M.; Spiess, B. *J. Am. Chem. Soc.* **2003**, *125*, 7768−7769.
(25) Dozol, H.; Blum-Held, C.; Guedat, P.; Maechling, C.; Lanners, S.; Schlewer, G.; Spiess, B. *J. Mol. Struct.* **2002**, *643*, 171−181.
(26) Liang, C. X.; Ewig, C. S.; Stouch, T. R.; Hagler, A. T. *J. Am. Chem. Soc.* **1994**, *116*, 3904−3911.
(27) Scheiner, S. *Hydrogen Bonding*; Oxford University Press: New York, 1997.
(28) Jeffrey, G. A. *An Introduction to Hydrogen Bond*; Oxford University Press: New York, 1997.
(29) Huggins, M. L. *Angew. Chem., Int. Ed. Engl.* **1971**, *10*, 147−152.
(30) Blum-Held, C.; Bernard, P.; Schlewer, G.; Spiess, B. *J. Am. Chem. Soc.* **2001**, *123*, 10788−10788.
(31) Kinser, R. D.; Nicol, G.; Ridge, D. P. *J. Phys. Chem. A* **2002**, *106*, 9925−9929.
(32) Karmacharya, R.; Antoniou, D.; Schwartz, S. D. *J. Phys. Chem. A* **2001**, *105*, 2563−2567.
(33) Brodskaya, E.; Lyubartsev, A. P.; Laaksonen, A. *J. Chem. Phys. B* **2002**, *106*, 6479−6487.

ods.[34] However, if the acidic part of the molecule or even the whole molecule is embedded in a protein, it is difficult to get an accurate pK_a experimentally. For some polyprotic acids, if the intermediate anions have a short lifetime, it is also hard to measure the exact pK_a values. In the case of a polyprotic acid, there may be several species contributing to an observed pK_a, so one needs to utilize the concept of microconstants in order to understand the dissociation equilibrium. It helps to discover the contribution of each acidic site to the observed pK_a.

Recent work has been dedicated to calculating accurate pK_a values theoretically[35−42] using the geometric and electronic structure information to estimate the pK_a values. Fairly accurate results have been gained for carboxylic acids and substituted phenols.[36,43−45] However, estimating the pK_a of diprotic acids (or polyprotic acids) remains a challenging problem, especially for organic phosphoric acids. To the best of our knowledge, no research has been done to date using quantum chemical calculations to predict absolute pK_a values of phosphoric acids which are involved in HBN. Ins(2)P_1 is a diprotic acid with two pK_a values. Due to intramolecular hydrogen bonding, the two protons are not equivalent. Specifically, the pK_a values of the monoanion, as a base and as an acid, are key to understanding the mechanisms of its reactions. In this paper, we report the absolute pK_a calculations of the two chair conformations and investigate the relationship between pK_a and conformations using first-principle methods.

This article is organized as follows. First, we concisely go over the computational methodology. Second, we discuss the intramolecular hydrogen bonding network for both neutral and deprotonated Ins(2)P_1. Third, we explore the transition states for the chair-to-chair inversion. Fourth, solvation effects on hydrogen bonding are discussed using implicit solvation methods as well as explicit water molecules. Fifth, the intramolecular proton migration and formation of four-center hydrogen bond in fully deprotonated Ins(2)P_1 are investigated. Finally, the pK_a values are determined and compared with experimental data.

Computational Methods

To determine the important thermally accessible local and global minima, a complete systematic conformational search was performed using HyperChem[46,47] with the MM+[47] force field by varying all torsion angles in the molecule with the restriction for maintaining the cyclohexane ring. The 30 lowest local minima from the conformational search were selected for further high-level geometry optimizations since these energies are within 6 kcal/mol of the global minimum and too close to be accurately ordered with the MM+ force field. For these selected conformations, the PM3, the Hartree−Fock, and density functional theory (DFT) methods using the 6-31G, 6-31G(d), and 6-31+G(d) basis sets[48] were performed to identify the global minimum. The effect of the different methods and the inclusion of polarization and diffuse basis orbitals are discussed for this particular molecule. For the DFT method, the Becke three-parameter hybrid functional combined with the Lee, Yang, and Parr correlation functional (B3LYP)[49] is employed. It includes a mixture of 20% Hartee−Fock exchange, the Becke exchange functional with nonlocal correlation provided by the LYP expression, and the VWN functional III for local correlation. Harmonic vibrational analyses are performed at the same level to confirm that the structure is a minimum or saddle point on the potential energy surface and to determine the enthalpy and free energy of each structure within the harmonic oscillator approximation.[50] The vibrational analyses are carried out on all optimized structures to get the thermochemical corrections to the energy and entropy due to vibrational, rotational, and translational degrees of freedom. All thermodynamic data were obtained at the standard state, i.e., 298.15 K and 1 atm. Additionally, the NMR chemical shift and coupling constants[51,52] were calculated on the fully optimized structures at the B3LYP/6-31+G(d) level. The NMR shielding results have been shown to give good agreement with experimental data[53] using this method. All DFT and ab initio calculations were carried out with the Gaussian 2003 program suite.[54]

The transition states were found for the chair-to-chair (1a/5e ⇌ 5a/1e) inversion. For large molecules such as Ins(2)P_1, it is difficult to find transition states directly because there are many groups with a variety of possible torsion conformations. We did the transition state search using the following strategy. We first calculated the saddle point for the ring inversion of cyclohexane and used it as a starting point for our target structure. Then, we added the phosphate and −OH groups to the cyclohexane ring to form Ins(2)P_1 to get our initial guess of the transition state structure. This structure was then partially optimized while constraining the ring configuration for the transition state. Finally, a full transition state optimization was carried out using the Synchronous Transit-Guided Quasi-Newton methods.[55,56] To verify each transition state, an intrinsic reaction coordinate (IRC)[57,58] calculation was completed as well as a frequency calculation which revealed only one imaginary frequency as validation of the transition state. Additional details about the optimized minima and transition state structures are shown in Table 1.

The *myo*-inositol phosphates easily dissolve in water due to the hydroxyl and phosphate groups. Since the chair-to-chair inversion is observed in experiments under aqueous environment, how the solvent affects the conformation is very important to clarify. In our calculations, we studied the solvation effects by using the polarized continuum model (PCM)[59−63] which was developed by Tomasi and co-workers. A dielectric constant of 78.39 is used. Due to convergence problems

(34) Cookson, R. F. *Chem. Rev.* **1974**, *74*, 5−28.
(35) Toth, A. M.; Liptak, M. D.; Phillips, D. L.; Shields, G. C. *J. Chem. Phys. A* **2001**, *114*, 4595−4606.
(36) Liptak, M. D.; Shields, G. C. *J. Am. Chem. Soc.* **2001**, *123*, 7314−7319.
(37) Abreu, H. A. D.; Almeida, W. B. D.; Duarte, H. A. *Chem. Phys. Lett.* **2004**, *383*, 47−52.
(38) Adam, K. R. *J. Phys. Chem. A* **2002**, *106*, 11963−11972.
(39) Topol, I. A.; Tawa, G. J.; Galdwell, R. A.; Eissenstat, M. A.; Burt, S. K. *J. Phys. Chem. A* **2000**, *104*, 9619−9624.
(40) Topol, I. A.; Tawa, G. J.; Burt, S. K.; Rashin, A. A. *J. Phys. Chem. A* **1997**, *101*, 10075−10081.
(41) Jang, Y. H.; Sowers, L. C.; Cagin, T.; Goddard, W. A. I. *J. Phys. Chem. A* **2001**, *105*, 274−280.
(42) Silva, C. O.; da Silva, E. C.; Nascimento, M. A. C. *J. Phys. Chem. A* **2000**, *104*, 2402−2409.
(43) Li, H.; Robertson, A. D.; Jensen, J. H. *Proteins: Struct., Funct., Bioinf.* **2004**, *55*, 689−704.
(44) Liptak, M. D.; Shields, G. C. *Int. J. Quantum Chem.* **2001**, *85*, 727−741.
(45) Liptak, M. D.; Gross, K. C.; Seybold, P. G.; Feldgus, S.; Shields, G. C. *J. Am. Chem. Soc.* **2002**, *124*, 6421−6427.
(46) Inc., H. *HyperChem*, release 6.01 ed.; Molecular Modeling System: Gainesville, FL, 2000.
(47) Allinger, N. L. *J. Am. Chem. Soc.* **1977**, *99*, 8127−8134.
(48) Hehre, W. J.; Radom, L.; Schlever, P. V. R.; Pople, J. A. *Ab Initio Molecular Orbital Theory*; Wiley: New York, 1986.
(49) Becke, A. D. *J. Chem. Phys. A* **1993**, *98*, 5648−5652.
(50) Cheeseman, J. R.; Frisch, M. J.; Devlin, F. J.; Stephens, P. J. *Chem. Phys. Lett.* **1996**, *252*, 211−220.
(51) Gauss, J. *J. Chem. Phys.* **1993**, *99*, 3629−3643.
(52) Gauss, J. *Phys. Chem. Chem. Phys* **1995**, *99*, 1001−1008.
(53) Alam, T. M. *Ab Initio Calculation of Nuclear Magnetic Resonance Chemical Shift Anisotropy*; Sandia National Laboratories, 1998.
(54) Frisch, M. J.; et al. *Gaussian 2003*; Pittsburgh, PA, 2003.
(55) Peng, C. Y.; Ayala, P. Y.; Schlegel, H. B.; Frisch, M. J. *J. Comput. Chem.* **1996**, *17*, 49−56.
(56) Peng, C. Y.; Schlegel, H. B. *Isr. J. Chem.* **1993**, *33*, 449−454.
(57) Gonzalez, C.; Schlegel, H. B. *J. Chem. Phys. A* **1989**, *90*, 2154−2161.
(58) Gonzalez, C.; Schlegel, H. B. *J. Phys. Chem. A* **1990**, *94*, 5523−5527.
(59) Miertus, S.; Scrocco, E.; Tomasi, J. *Chem. Phys.* **1981**, *55*, 117−129.
(60) Cossi, M.; Barone, V.; Cammi, R.; Tomasi, J. *Chem. Phys. Lett.* **1996**, *255*, 327−335.
(61) Barone, V.; Cossi, M.; Mennucci, B.; Tomasi, J. *J. Chem. Phys. A* **1997**, *107*, 3210−3221.
(62) Cances, M. T.; Mennucci, B.; Tomasi, J. *J. Chem. Phys. A* **1997**, *107*, 3032−3041.
(63) Barone, V.; Cossi, M.; Tomasi, J. *J. Comput. Chem.* **1998**, *19*, 404−417.

Table 1. 1a/5e, 5a/1e, and Transition State Conformations of *myo*-Inositol, Ins(2)P_1^0 and Its Anions Ins(2)P_1^{1-} and Ins(2)P_1^{2-}[a]

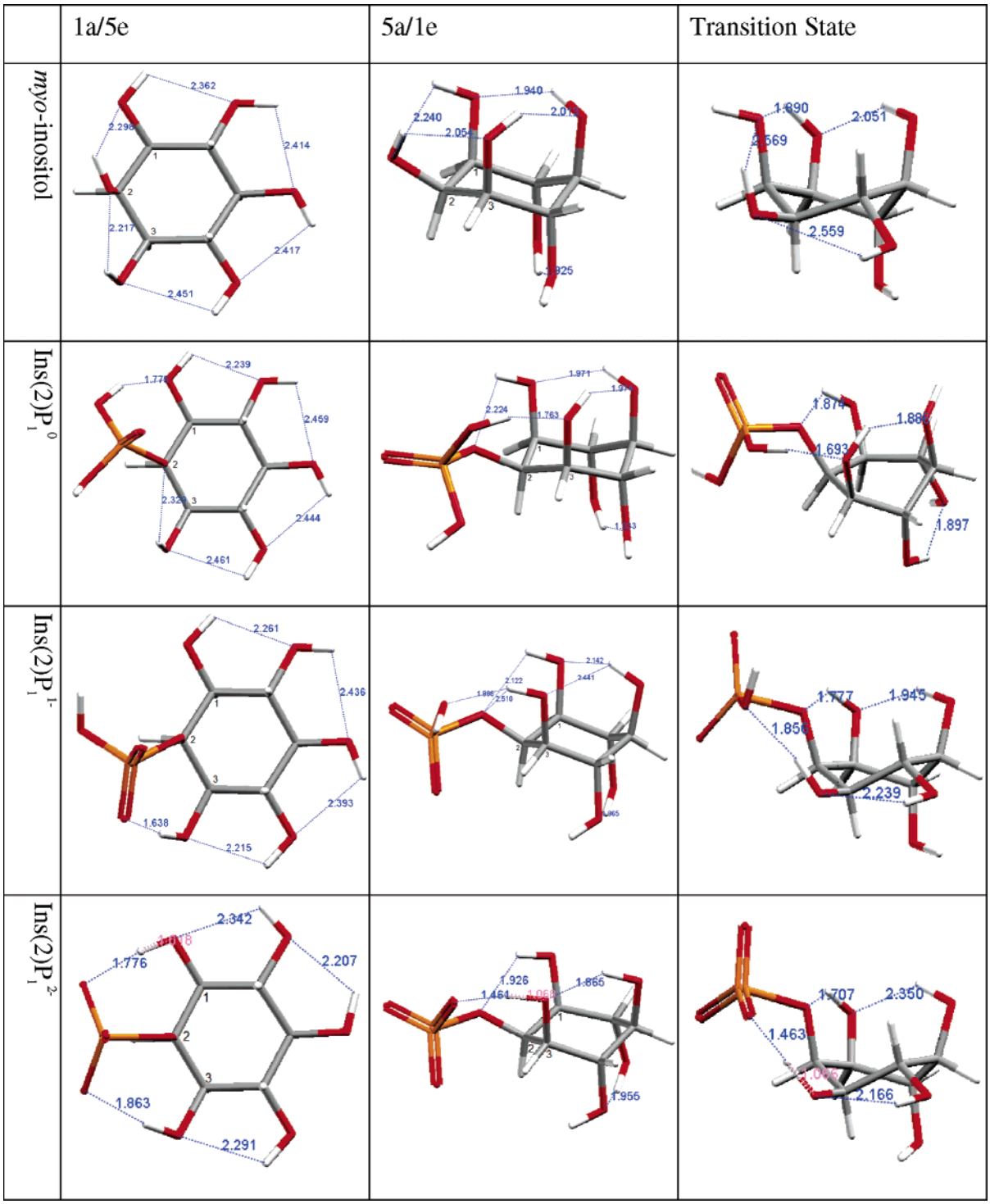

[a] Phosphorus (oxygen) atoms are shown in gold (red). Carbon (hydrogen) atoms are shown in gray (white).

associated with optimization in solution, the solvent phase calculations were completed at the gas phase optimized geometries. It has been shown that the free energy of solvation can be accurately computed also using the in vacuo optimized geometry at the same level of theory.[61] For the SCRF[64,65] method, the radius of each atom in the molecule was calculated using the United Atom Topological Model. One concern is that the intermolecular hydrogen bonding with solvent molecules may affect the conformation of inositol phosphates by breaking up the intramolecular hydrogen bonding network to form hydrogen bonds with solvent molecules. A semiempirical molecular dynamics simulation (a trajectory calculation using the Atom Centered Density Matrix Propagation molecular dynamics model[66−68]) at the PM3 level for Ins(2)P_1 surrounded by 14 water molecules as the first layer of solvent shell

(64) Cammi, R.; Mennucci, B.; Tomasi, J. *J. Phys. Chem. A* **2000**, *104*, 5631−5637.
(65) Cammi, R.; Mennucci, B.; Tomasi, J. *J. Phys. Chem. A* **1999**, *103*, 9100−9108.
(66) Schlegel, H. B.; Iyengar, S. S.; Li, X.; Millam, J. M.; Voth, G. A.; Scuseria, G. E.; Frisch, M. J. *J. Chem. Phys.* **2002**, *117*, 8694−8704.
(67) Schlegel, H. B.; Millam, J. M.; Iyengar, S. S.; Voth, G. A.; Daniels, A. D.; Scuseria, G. E.; Frisch, M. J. *J. Chem. Phys.* **2001**, *114*, 9758−9763.
(68) Iyengar, S. S.; Schlegel, H. B.; Millam, J. M.; Voth, G. A.; Scuseria, G. E.; Frisch, M. J. *J. Chem. Phys.* **2001**, *115*, 10291−10302.

was completed. This reveals that the solvent molecules do not destroy the intramolecular hydrogen bonds and so do not have a noticeable effect on the conformational preference of Ins(2)P_1. An ab initio molecular dynamics simulation at the B3LYP/6-31+G(d) level is computationally unfeasible for such a large system. The crystal structure[69] shows that four water molecules could form hydrogen bonds with Ins(2)P_1. For the thermally favorable 1a/5e conformations, we investigated the interference from these explicit water molecules by fully optimizing each complex of Ins(2)P_1^0, Ins(2)P_1^{1-}, and Ins(2)P_1^{2-} with four water molecules at the B3LYP/6-31+G(d) level. These results indicate that these imbedded water molecules do not break up the intramolecular hydrogen bonding network.

The evaluation of the absolute pK_a values from quantum chemical calculations is a subject of intense interest and also one that presents considerable challenges. It is complicated by some uncertainty regarding both the theoretical treatment and the experimental value for the solvation energy of the proton.[70,71] There are several computational methods developed[38,71−74] in the past decade. Sprik and co-workers used a statistical mechanical method described by Chandler[75] to predict pK_a values of pentaoxyphosphoranes.[76] Shields[36] proposed a method avoiding the precise determination of the proton solvation free energy which still has a considerable experimental uncertainty.[33,77] Our calculations follow the thermodynamic cycle shown in Figure 3: the solute molecule (acid) is taken out of solution and dissociated in a vacuum, and then the fragments are finally reinserted into solution.

The free energy of dissociation in solution can be decomposed into the corresponding reaction in gas phase, ΔG_g, and the sum of the free energy of solvation for each species.

$$\Delta G_s^\circ = G^\circ(A_{aq}^-) + G^\circ(H_{aq}^+) - G^\circ(HA_{aq})$$
$$= \Delta G_g^\circ + \Delta G_s^\circ(A^-) + \Delta G_s^\circ(H^+) - \Delta G_s^\circ(HA)$$
$$= \Delta G_g + \Delta\Delta G_s$$

where

$$\Delta G_g = G^\circ(A_g^-) + G^\circ(H_g^+) - G^\circ(HA_g)$$
$$\Delta\Delta G_s = \Delta G_s^\circ(A^-) + \Delta G_s^\circ(H^+) - \Delta G_s^\circ(HA)$$

The equilibrium constant K_a of the aqueous reaction is closely related to the dissociation free energy change by the following equations.

$$pK_a = -\log K_a$$
$$\Delta G_s^\circ = -2.303RT \log K_a$$
$$pK_a = \Delta G_s^\circ/2.303RT$$

It is assumed that concentrations can be used instead of activities in the above equations. Or, it is not necessary to explicitly include the activity coefficients, because all physically relevant solute−solvent interactions are included in the solvation free energy ΔG_s°. When the solvation free energy change ΔG_s° is defined for a 1 M solution at 298 K and 1 atm, the Gibbs free energy of the proton is $G^\circ(H_g^+) = 2.5RT - T\Delta S^\circ = 1.48 - 7.76 = -6.28$ kcal/mol as taken from the literature.[39,40,78] The free energy of solvation of a proton in water is of fundamental importance to the accuracy of pK_a calculations. The most recent studies on the accurate free energy of hydration of ions give a theoretical value of $\Delta G_s^\circ(H^+)$ between −264.1 and −264.3 kcal/mol,[79,80] for a standard state concentration of 1 M. This result agrees with the experimental value of $\Delta G_s^\circ(H^+) = -263.98 \pm 0.07$ kcal/mol.[81] In our calculations, the value of $\Delta G_s^\circ(H^+) = -264.0$ kcal/mol is used to obtain the pK_a of Ins(2)P_1.

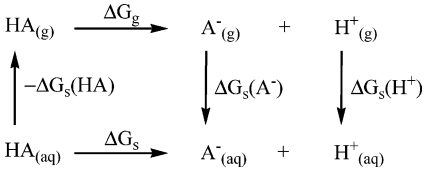

Figure 3. Thermodynamic cycle used to evaluate pK_a values by the absolute method.

Results and Discussion

I. Structural Results. The global minimum for the neutral Ins(2)P_1 takes the 1a/5e structure where the phosphate group is in the axial position with all −OH groups in the equatorial positions. Similarly, the partially ionized Ins(2)P_1^{1-} and the fully ionized Ins(2)P_1^{2-} compounds also adopt the 1a/5e conformation as the global minima. The corresponding chair form after ring inversion for neutral Ins(2)P_1 is shown in Table 1 where the phosphate group is in the equatorial position while the −OH groups are in axial positions. Intramolecular hydrogen bonds are formed in all conformations to lower the energies and stabilize the structures.

I.1. *myo*-Inositol. In the 1a/5e conformation of *myo*-inositol, which has 6.683 kcal/mol lower energy than the corresponding 5a/1e conformation, there exist six hydrogen bonds, ranging from 2.217 to 2.451 Å, forming a closed ring of hydrogen bonds outside the cyclohexane ring. Each hydrogen bond is part of a five-member ring. All the hydroxyl bonds connect to each other head-to-tail in a zigzag pattern and point in the same direction (clockwise for O−H···O when viewed from above the ring on the side of the axial 2 position). The formation of this unidirectional network of hydrogen bonds takes advantage of many-body nonadditive interactions known as hydrogen bond cooperativity.[28] The similar cooperativity is found in the 5a/1e conformation, as shown in Table 1. Four hydrogen bonds are above the ring and are shorter than those in the 1a/5e conformation. The preferred chair conformation found here is consistent with experimental observation.[82] The hydrogen bond network is the main factor that determines the conformational preference in *myo*-inositol. *myo*-Inositol headgroups are common to membrane phospholipids, and although many factors may effect their conformations, these results imply that cooperative hydrogen bonding networks may be an important factor in these more complex systems.

I.2. Ins(2)P_1^0. The replacement of one hydroxyl group by one phosphate group in the *myo*-inositol molecule does not affect the pattern of the HBN but enforces the strength of hydrogen

(69) Yoo, C. S.; Blank, G.; Pletcher, J.; Sax, M. *Acta Crystallogr., Sect. B* **1974**, *30*, 1983−1987.
(70) Lano, J.; Eriksson, L. A. *J. Chem. Phys.* **2002**, *117*, 10193−10206.
(71) Chipman, D. M. *J. Phys. Chem. A* **2002**, *106*, 7413−7422.
(72) J. R. Pliego, J. *Chem. Phys. Lett.* **2003**, *367*, 145−149.
(73) Pliego, J. R.; Riveros, J. M. *J. Phys. Chem. A* **2002**, *106*, 7434−7439.
(74) Jang, Y. H.; Goddard, W. A., III; Noyes, K. T.; Sowers, L. C.; Hwang, S.; Chung, D. S. *J. Phys. Chem. B* **2003**, *107*, 344−357.
(75) Chandler, D. *Introduction to Modern Statistical Mechanics*; Oxford University Press: Oxford, 1987.
(76) Davies, J. E.; Doltsinis, N. L.; Kirby, A. J.; Roussev, C. D.; Sprik, M. *J. Am. Chem. Soc.* **2002**, *124*, 6594−6599.
(77) Mejias, J. A.; Lago, S. *J. Chem. Phys. A* **2000**, *113*, 7306−7316.
(78) Lim, C.; Bashford, D.; Karplus, M. *J. Phys. Chem. A* **1991**, *95*, 5610−5620.
(79) Tawa, G. J.; Topol, I. A.; Burt, S. K.; Caldwell, R. A.; Rashin, A. A. *J. Chem. Phys.* **1998**, *109*, 4852−4863.
(80) Zhan, C. G.; Dixon, D. A. *J. Phys. Chem. A* **2001**, *105*, 11534−11540.
(81) Tissandier, M. D.; Cowen, K. A.; Feng, W. Y.; Gunglach, E.; Chen, M. H.; Earhart, A. D.; Coe, J. V.; Turrle, T. R. *J. Phys. Chem. A* **1998**, *102*, 7787−7794.
(82) IUPAC *Biochem. J.* **1989**, *258*, 1−2.

Table 2. Hydrogen Bonds of the 1a/5e, 5a/1e, and Transition State (TS) Conformations of Ins(2)$P_1{}^0$

1a/5e Conformation

	$O^{28}—H^{29}- - -O^7$		$O^7—H^{19}- - -O^{12}$		$O^{12}—H^{24}- - -O^{11}$		$O^{11}—H^{23}- - -O^{10}$		$O^{10}—H^{22}- - -O^9$		$O^9—H^{21}- - -O^8$	
	length, Å	angle, deg	length, Å	angle deg	length, Å	angle deg	length, Å	angle deg	length, Å	angle deg	length, Å	angle deg
HF/6-31G	2.03	125.5	2.364	105.5	2.51	99.1	2.487	100.5	2.566	99.8	2.26	107.2
HF/6-31G(d)	1.94	141.2	2.28	109.4	2.43	102.7	2.43	103.8	2.46	104.4	2.31	108.8
HF/6-31+G(d)	1.97	140.2	2.31	107.9	2.46	101.6	2.45	102.6	2.48	102.9	2.34	107.6
B3LYP/6-31G(d)	1.77	151.7	2.20	113.5	2.43	104.6	2.41	106.9	2.41	108.3	2.27	111.6
B3LYP/6-31G+(d)	1.77	153.2	2.239	111.3	2.459	103.1	2.44	104.6	2.46	105.5	2.328	109.6

5a/1e Conformation

	$H^{19}—O^7- - -O^8$		$H^{23}—O^{11}- - -O^7$		$H^{22}—O^{10}- - -O^{11}$		$H^{27}—O^{26}- - -O^9$		$O^{12}—H^{24}- - -O^{10}$	
	length, Å	angle, deg	length, Å	angle deg	length, Å	angle deg	length, Å	angle deg	length, Å	angle deg
HF/6-31G	2.325	100.84	2.06	122.27	2.05	133.70	1.778	149.47	1.939	136.02
HF/6-31G(d)	2.308	103.35	2.347	108.14	2.117	131.90	1.882	153.53	2.00	138.58
HF/6-31+G(d)	2.34	101.70	2.356	108.63	2.134	131.47	1.89	153.36	2.02	137.51
B3LYP/6-31G(d)	2.16	112.06	1.89	139.1	1.915	142.73	1.744	156.0	1.892	142.57
B3LYP/6-31G+(d)	2.224	108.95	1.970	134.00	1.974	140.02	1.76	157.44	1.933	140.41

Transition State (TS)

	$O^7—H^{19}- - -O^8$		$O^9—H^{21}- - -O^{11}$		$O^{26}—H^{27}- - -O^9$		$O^{10}—H^{22}- - -O^{12}$	
	length, Å	angle, deg	length, Å	angle deg	length, Å	angle deg	length, Å	angle deg
HF/6-31G	1.919	117.47	1.821	136.03	1.740	149.05	2.113	126.39
HF/6-31G(d)	1.93	118.62	1.916	134.51	1.856	153.21	2.11	129.85
HF/6-31+G(d)	1.935	118.57	1.937	133.63	1.846	154.10	2.132	129.60
B3LYP/6-31G(d)	1.833	123.75	1.897	134.42	1.68	156.37	1.857	146.82
B3LYP/6-31G+(d)	1.874	122.01	1.886	134.31	1.693	155.89	1.897	141.58

bonds within the network. Similar to *myo*-inositol, there are six hydrogen bonds in the 1a/5e conformation of Ins(2)$P_1{}^0$, the global minimum. The strongest hydrogen bond has a length (H···O) of 1.77 Å (based on the B3LYP/6-31+G(d) calculation) formed between the oxygen of the 1-hydroxyl group and the hydrogen of the phosphate group. The other five weaker hydrogen bonds have lengths between 2.24 and 2.46 Å, and all are in a five-member ring formed with its vicinal hydroxyl group. All the hydroxyl bonds connect to each other head-to-tail in a zigzag pattern and point in the same direction (clockwise for O−H···O when viewed from the phosphate side of the ring) to form a closed ring of hydrogen bonds outside the cyclohexane ring. In general, this type of hydrogen-bonding networks can be classified as homodromic (i.e., exhibiting a cyclic sequential donor−acceptor arrangement).[83]

There are five hydrogen bonds in the 5a/1e conformation, in which the shortest hydrogen bond length is 1.76 Å and between the oxygen of the phosphate group and the ^{3}OH group. Four of these hydrogen bonds are orientated counterclockwise to form a ring on top of the cyclohexane ring with lengths from 1.93 to 2.24 Å and benefit from the hydrogen bond cooperativity, while the fifth one is between the ^{4}OH and ^{6}OH hydroxyl groups on the opposing side of the cyclohexane ring. For all five-member rings, the hydrogen bond angles are about 105° (±5°); for the rings with six or more members, the hydrogen bond angles are about 140°. The information on these hydrogen bonds is available in Table 2 (see Supporting Information for the numbering of the atoms in Ins(2)P_1).

Although the average hydrogen bond length of the 5a/1e conformation is 0.36 Å shorter than that for the 1a/5e conformation, the 1a/5e conformation has a lower energy (7.56 kcal/mol with ZPE correction) than the corresponding 5a/1e conformation due to one more hydrogen bond and less steric interaction. In both structures, there is no significant difference among the O−H···O angles for all hydrogen bonds. The preference of the 1a/5e conformation of Ins(2)$P_1{}^0$ implies that phosphatidylinositol, which is a membrane lipid and has a *myo*-inositol as a polar headgroup,[84] may adopt the same stable conformation. These inositol-containing headgroups might somehow be linked to vesicle trafficking.[85]

The calculated gas-phase energy difference between these two structures varies from 4.75 to 8.64 kcal/mol depending on the level of calculation (Table 5). The energy difference is about the same order as one hydrogen bond energy in vacuo and varies depending on the basis set regardless of the method. With improvement of the basis set [6-31G(d), 6-31G(d), 6-31+G-(d)], the energy difference gets larger both in vacuo and aqueous solution. The polarization functions are important due to the softness (polarizability) of the phosphorus atom. The diffuse functions are essential even for this neutral system because of the partially charged phosphate group. Thus, the addition of extra polarization and diffuse function gives better energy prediction. However, the hydrogen bond lengths and the bond angles increase only slightly and are not sensitive to the size of the basis sets. Usually, the DFT methods give shorter hydrogen bond lengths and larger O−H···O angles than the HF methods with the inclusion of electronic correlation in DFT methods.

Depending on the level of the calculation, the dipole moment of the 5a/1e conformation is 1.6−2.0 times that of the 1a/5e

(83) Saenger, W. *Nature (London)* **1979**, *279*, 343−344.
(84) Koga, Y.; Nishihara, M.; Morii, H.; Akagawa-Matsushita, M. *Microbiol. Rev.* **1993**, *57*, 164−182.
(85) Martin, T. F. *Curr. Opin. Neurobiol.* **1997**, *7*, 331−338.

Table 3. Hydrogen Bonds of the 1a/5e, 5a/1e, and Transition State (TS) Conformations of Ins(2)P_1^{1-}

1a/5e Conformation

	$O^7—H^{19}- - -O^{12}$		$O^{12}—H^{24}- - -O^{11}$		$O^{11}—H^{23}- - -O^{10}$		$O^{10}—H^{22}- - -O^9$		$O^9—H^{21}- - -O^{26}$	
	length, Å	angle, deg	length, Å	angle, deg	length, Å	angle, deg	length, Å	angle, deg	length, Å	angle, deg
HF/6-31G	2.35	107.4	2.475	101.6	2.434	104.9	2.36	106.8	1.718	166.2
HF/6-31G(d)	2.278	111.2	2.419	104.4	2.366	108.6	2.27	111.0	1.739	168.6
HF/6-31+G(d)	2.30	109.7	2.44	103.1	2.387	107.2	2.296	109.5	1.745	168.1
B3LYP/6-31G(d)	2.22	115.1	2.40	107.1	2.366	111.3	2.14	117.9	1.62	170.7
B3LYP/6-31G+(d)	2.261	112.73	2.436	105.11	2.393	109.27	2.215	114.53	1.638	171.00

5a/1e Conformation

	$O^7—H^{19}- - -O^8$		$O^{11}—H^{23}- - -O^7$		$O^{11}—H^{23}- - -O^9$		$O^9—H^{21}- - -O^8$		$O^9—H^{21}- - -O^{26}$		$O^{12}—H^{24}- - -O^{10}$	
	length, Å	angle, deg	length, Å	angle, deg	length, Å	angle, deg	length, Å	angle, deg	length, Å	angle, deg	length, Å	angle, deg
HF/ 6-31G	2.200	106.15	1.985	135.76	2.115[a]	145.02	2.328 (O^7)[b]	125.51	2.581 (O^{11})[c]	112.65	1.968	137.05
HF/ 6-31G(d)	2.149	113.39	2.228	126.70	2.332	119.08	2.452	100.00	2.047	148.37	2.017	139.54
HF/ 6-31+G(d)	2.174	112.02	2.272	125.17	2.361	118.57	2.491	98.35	2.062	147.65	2.043	138.09
B3LYP/ 6-31G(d)	2.081	117.87	2.043	135.53	2.419	113.85	2.450	100.23	1.860	156.77	1.916	145.03
B3LYP/ 6-31G+(d)	2.122	115.59	2.145	131.05	2.441	114.85	2.511	98.06	1.888	154.64	1.965	142.14

Transition State (TS)

	$H^{19}—O^7- - -O^8$		$O^{11}—H^{23}- - -O^7$		$O^{10}—H^{22}- - -O^9$		$O^9—H^{21}- - -O^{26}$	
	length, Å	angle, deg	length, Å	angle, deg	length, Å	angle, deg	length, Å	angle, deg
HF/6-31G	1.911	117.02	2.182	133.88	2.423	106.22	1.832	167.05
HF/6-31G(d)	1.916	118.87	2.158	137.71	2.353	110.38	2.023	168.26
HF/6-31+G(d)	1.938	117.90	2.245	134.25	2.369	109.01	1.994	168.77
B3LYP/6-31G(d)	1.777	126.50	1.945	146.60	2.239	115.87	1.856	168.04
B3LYP/6-31G+(d)	1.777	126.50	1.945	146.60	2.239	115.87	1.856	168.04

[a] Hydrogen bond for $O^{26}—H^{27}- - -O.^9$ [b] Hydrogen bond for $O^9—H^{21}- - -O^7$. [c] Hydrogen bond for $O^9—H^{21}- - -O^{11}$.

conformation for both the gas and aqueous phases. As the size of the basis set increases, the dipole moment of each optimized structure increases slightly. For every optimized molecule, the solvent effect increases the dipole moment as is normally expected. The solvent induced dipole moment for the 1a/5e conformation contributes about 30% of the total dipole moment at all levels of theory, while that for the 5a/1e conformation is 20% and 26%, respectively, for the HF and DFT methods. The significance of the solvent induced component of the dipole moment can be calculated by $(D_s - D_g)/D_g * 100\%$. Due to the flatter and larger surface area of the 1a/5e conformation, the solvent has a larger effect than for the 5a/1e conformation.

I.3. Ins(2)P_1^{1-}. Due to the acidity of the phosphoric acid group in Ins(2)P_1^0, the concentration of Ins(2)P_1^0 is very low in biological systems. Under actual physiological conditions, *myo*-inositol phosphates exist in the deprotonated forms. Most reactions involving the phosphate group act in response to partially or fully deprotonated species. Accordingly, the effect of deprotonation on HBN is an important subject for many biological reactions.

When the 1a/5e conformation of Ins(2)P_1^0 deprotonates to form Ins(2)P_1^{1-}, it is highly likely that the non-hydrogen-bonded hydrogen on the phosphoric acid group is lost. After the proton is lost, the newly formed oxygen ion has a large net charge and can attach to the hydrogen of the vicinal ^{3}OH hydroxyl group to form a new strong hydrogen bond. This new hydrogen bond between the phosphate $P—O^-$ oxygen and the hydrogen of the ^{3}OH group becomes the strongest with a H···O distance of 1.64 Å (Table 3). The other four hydrogen bonds in Ins(2)P_1^{1-} are the same as those in the 1a/5e conformation of Ins(2)P_1^0 except that the hydrogen bond to the ^{1}OH hydroxyl group is lost and the one to the ^{3}OH hydroxyl group shifts to the deprotonated oxygen ion on the phosphate group from the phosphoester oxygen atom. The partially deprotonated form has one hydrogen bond less than the neutral form, but the pattern of the hydrogen bonds is similar to that in the 1a/5e conformation of neutral Ins(2)P_1.

In a manner similar to the formation of the 1a/5e conformation of Ins(2)P_1^{1-}, the loss of the non-hydrogen bonded hydrogen in the 5a/1e conformation of Ins(2)P_1^0 gives the global minimum for this conformation of Ins(2)P_1^{1-}. Although there are five hydrogen bonds in the neutral species, six hydrogen bonds are formed in the 5a/1e conformation of Ins(2)P_1^{1-}. The hydrogen atom of the ^{5}OH group and the phosphoester oxygen are involved in two hydrogen bonds simultaneously to form a three-centered configuration, while the hydrogen atom of ^{3}OH group forms a chelated one.

The hydrogen bonds are not oriented cyclically in the same direction as in the neutral species, since the ^{5}OH hydroxyl group points to the center of the cyclohexane ring. Although there is one more hydrogen bond formed in the 5a/1e conformation, its energy is higher than that for the 1a/5e conformation possibly due to the lengthening of the hydrogen bonds and the higher steric stress of the four-member ring involving two hydrogen bonds to the hydrogen of the ^{3}OH hydroxyl group. The effect of basis sets and methods on the hydrogen bond lengths and bond angles is the same as that with Ins(2)P_1^0.

With the loss of one proton, the dipole moment of Ins(2)P_1^{1-} is over three times larger than that for Ins(2)P_1^0, while that of 1a/5e is twice as large as the respective one for the 5a/1e

Table 4. Hydrogen Bonds of the 1a/5e, 5a/1e, and Transition State (TS) Conformations of Ins(2)P_1^{2-}

1a/5e Conformation

	$O^7—H^{19}- - -O^{28}$		$O^{12}—H^{24}- - -O^7$		$O^{11}—H^{23}- - -O^{12}$		$O^{10}—H^{22}- - -O^9$		$O^9—H^{21}- - -O^{26}$	
	length, Å	angle, deg	length, Å	angle, deg	length, Å	angle, deg	length, Å	angle, deg	length, Å	angle, deg
HF/6-31G	1.790	165.68	2.405	107.73	2.273	111.08	2.365	108.84	1.871	164.76
HF/6-31G(d)	1.851	167.19	2.330	111.33	2.224	114.63	2.289	113.08	1.922	166.09
HF/6-31+G(d)	1.888	166.54	2.351	109.85	2.249	113.12	2.316	111.35	1.963	165.56
B3LYP/6-31G(d)	1.727	169.08	2.291	115.45	2.162	119.22	2.228	118.182	1.801	167.79
B3LYP/6-31G+(d)	1.776	168.88	2.342	112.70	2.207	116.49	2.291	114.83	1.863	167.55

5a/1e Conformation

	$O^7—H^{19}- - -O^8$		$O^7- - -H^{23}—O^{11}$		$O^9- - -H^{23}—O^{11}$		$O^9—H^{21}- - -O^{26}$		$O^{12}—H^{24}- - -O^{10}$		$O^{10}—H^{22}- - -O^{26}$	
	length, Å	angle, deg	length, Å	angle, deg	length, Å	angle, deg	length, Å	angle, deg	length, Å	angle, deg	length, Å	angle, deg
HF/6-31G	2.038	116.62	2.646	106.92	1.951	135.92	1.577	158.26	1.992	138.12	- - - - -	- - - - -
HF/6-31G(d)	2.014	119.69	2.505	112.99	2.044	134.95	1.628	159.77	2.023	139.98	- - - - -	- - - - -
HF/6-31+G(d)	2.018	118.46	2.499	116.38	2.163	129.20	2.131 (O^8)[a]	113.69 (O^8)[a]	2.086	136.11	- - - - -	- - - - -
B3LYP/6-31G(d)	1.842 (O^9)[b]	139.76 (O^9)[b]	1.913	147.17	- - - - -	- - - - -	1.959 (O^{11})[c]	137.58 (O^{11})[c]	1.966	146.72	1.534	169.35
B3LYP/6-31G+(d)	1.926	123.1	- - - - -	- - - - -	1.865	143.5	1.461	165.3	1.955	143.1	- - - - -	- - - - -

Transition State (TS)

	$H^{19}—O^7- - -O^8$		$O^{11}—H^{23}- - -O^7$		$O^{10}—H^{22}- - -O^9$		$O^9—H^{21}- - -O^{28}$	
	angle, deg	length, Å	angle, deg	length, Å	angle, deg	length, Å	angle, deg	length, Å
HF/6-31G	1.769	123.77	2.132	134.58	2.237	111.56	1.508	172.02
HF/6-31G(d)	1.773	126.02	2.188	135.85	2.185	115.22	1.584	174.91
HF/6-31+G(d)	1.805	124.19	2.275	132.30	2.231	112.84	1.625	173.72
B3LYP/6-31G(d)	1.770	129.19	2.370	140.10	2.229	124.16	1.406	173.98
B3LYP/6-31G+(d)	1.707	129.51	2.350	131.34	2.166	117.81	1.463	176.41

[a] Hydrogen bond for $O^9—H^{21}\cdots O^8$. [b] Hydrogen bond for $O^7—H^{19}\cdots O^9$. [c] Hydrogen bond for $O^9—H^{21}\cdots O^{11}$.

conformation of Ins(2)P_1^0. This can be explained by the optimized structure. The hydrogen bonds of the 5a/1e conformation all point to the phosphate group which compensates its anion charge to better distribute the charge of the molecule than in the 1a/5e conformation whose hydrogen bonds have a cyclic or more symmetric orientation.

At all levels of theory, the relative difference of the dipole moments between the two conformations is smaller compared to the neutral species. As with Ins(2)P_1^0, each optimized structure's dipole moment increases slightly upon increasing the size of the basis set. The solvent induced component of the dipole moment for the 1a/5e conformation contributes about 20% of the total dipole moment at all levels of theory, while that for the 5a/1e conformation contributes 17% and 24%, respectively, for the HF and DFT methods. Solvation effects make the energy difference between the two chair forms vary only about ±3 kcal/mol from those calculated in vacuo.

I.4. Ins(2)P_1^{2-}. When the partially deprotonated Ins(2)P_1^{1-} loses one more hydrogen to form the fully deprotonated Ins(2)P_1^{2-}, the oxygen atoms of the phosphate group become more prone to forming hydrogen bonds because of the high charge distribution. To form a strong hydrogen bond between the phosphate group and the ^{1}OH hydroxyl group, the unidirectional orientation of the cyclic hydrogen bond network is broken up. The hydrogen bond directions are no longer unidirectional but orient so that all hydrogen bonds point toward the anionic phosphate group. Those of the ^{4}OH and ^{3}OH hydroxyl groups are clockwise, while those of the ^{1}OH, ^{6}OH, and ^{5}OH hydroxyl groups are counterclockwise. These two sub-unidirectional hydrogen bond groups also take some advantage of cooperativity. Hydrogen bonding has a significant electrostatic component to balance the charge on the phosphate group. There are still five hydrogen bonds in the 1a/5e conformation which is the same as in the 1a/5e conformation of Ins(2)P_1^{1-}. But Ins(2)P_1^{2-} has two relatively short and strong hydrogen bonds between the phosphate group and the vicinal ^{1}OH and ^{3}OH hydroxyl groups.

In the fully deprotonated 5a/1e conformation, there are a total of four H-bonds. The stabilized conformation also indicates a very weak H-bond between ^{5}OH and ^{1}OH with a H···O distance of 2.783 Å (Table 4). A very short hydrogen bond with a length of 1.46 Å is formed between the phosphate group and ^{3}OH group. The O−H bond length of the ^{3}OH hydroxyl group is lengthened by 0.088 Å due to this short hydrogen bond. It should be mentioned here that the proton transfer could happen in fully deprotonated species due to the formation of this strong hydrogen bond. This possibility of intramolecular proton transfer through the hydrogen bond is another important artifact of the HBN.

With a lengthened O−H bond and a less symmetric structure, the 5a/1e conformation has a higher energy than the 1a/5e conformation. The effects of changing the basis set and the level of theory are similar to those found for Ins(2)P_1^0.

Compared with Ins(2)P_1^0 and Ins(2)P_1^{1-}, the dipole moment difference between the two chair forms of Ins(2)P_1^{2-} is noticeably smaller resulting in dipole moments that are nearly equal (Table 5). This could be explained by having the clockwise direction of hydrogen bonds in 1a/5e broken with all hydrogen

Table 5. Energy Difference between 1a/5e and 5a/1e [$E_{(1a/5e)} - E_{(5a/1e)}$ (kcal/mol)], Activation Energy of the 1a/5e Conformation (kcal/mol), and Dipole Moment for the Optimized Structures (Debye)

Energy Difference between 1a/5e and 5a/1e

	Ins(2)P_1^0		Ins(2)P_1^{1-}		Ins(2)P_1^{2-}	
	vacuo	aqueous	vacuo	aqueous	vacuo	aqueous
HF/6-31G	−4.75	−4.52	−8.47	−5.50	−4.42	−4.65
HF/6-31G(d)	−6.98	−5.68	−4.44	−6.80	−6.60	−8.26
HF/6-31+G(d)	−8.64	−8.20	−6.54	−9.59	−15.97	−13.98
B3LYP/6-31G(d)	−4.83	−3.79	−2.98	−4.63	−3.23	−4.52
B3LYP/6-31+G(d)	−7.56	−8.11	−6.17	−8.53	−4.56	−7.53

Activation Energy of 1a/5e

	Ins(2)P_1^0		Ins(2)P_1^{1-}		Ins(2)P_1^{2-}	
	vacuo	aqueous	vacuo	aqueous	vacuo	aqueous
HF/6-31G	18.56	17.58	10.13	13.54	11.12	13.67
HF/6-31G(d)	21.83	21.10	11.33	15.56	12.49	15.60
HF/6-31+G(d)	22.22	22.13	12.22	16.48	12.57	15.46
B3LYP/6-31G(d)	17.07	14.99	7.55	11.49	5.61	8.53
B3LYP/6-31+G(d)	18.53	18.16	10.51	15.62	6.37	12.48

Dipole Moment for Optimized Structures

	Ins(2)P_1^0			Ins(2)P_1^{1-}			Ins(2)P_1^{2-}		
	1a/5e	5a/1e	TS	1a/5e	5a/1e	TS	1a/5e	5a/1e	TS
HF/6-31G	2.47[a]	6.65	7.43	11.26	12.09	8.05	13.99	14.58	14.93
	(3.63)[b]	(8.04)	(8.93)	(13.55)	(13.94)	(9.63)	(16.91)	(17.26)	(17.78)
HF/6-31G(d)	2.79	5.14	6.06	10.29	7.53	8.29	14.23	14.34	14.26
	(3.63)	(6.05)	(7.26)	(12.38)	(8.83)	(9.95)	(17.17)	(17.02)	(17.10)
HF/6-31+G(d)	2.92	5.43	6.22	10.30	7.80	8.54	14.94	16.61	14.85
	(3.86)	(6.48)	(7.53)	(12.61)	(9.26)	(10.37)	(18.16)	(19.30)	(17.97)
B3LYP/6-31G(d)	2.77	4.55	5.44	9.11	6.50	6.97	12.28	14.63	10.06
	(3.66)	(5.72)	(6.86)	(11.37)	(8.00)	(8.71)	(15.54)	(18.58)	(12.99)
B3LYP/6-31+G(d)	3.15	5.03	5.48	9.26	6.98	7.14	13.40	13.22	12.80
	(4.25)	(6.41)	(7.03)	(11.85)	(8.72)	(9.14)	(17.11)	(16.72)	(16.43)

[a] The dipole moment in gas phase. [b] The dipole moment in aqueous phase.

bonds pointing toward the phosphate group. For both chair forms, the solvent induced dipole moment contributes around 20% and 27%, respectively, for the HF and DFT methods regardless of the basis set size.

Experimental ^{1}H NMR data of Ins(2)P_1 by Spiess et al.[24] show that the protons of the hydroxyl groups vicinal to the phosphate group gave broad signals at 6.9 ppm which appeared at pH 9.7 and pH 10.4 when Ins(2)P_1 was fully deprotonated. Our calculated NMR data, i.e., the chemical shift, for the global minima (1a/5e conformation) of Ins(2)P_1^0, Ins(2)P_1^{1-}, and Ins(2)P_1^{2-} are supported by the experimental values. Peaks were predicted at 6.97 and 6.16 ppm for ^{1}OH and ^{3}OH, respectively, for the Ins(2)P_1^{2-} anion and 6.72 ppm for ^{3}OH of Ins(2)P_1^{1-}, while no such downfield chemical shift was found for the neutral species. Additionally, the experiment was ran using an 80% H_2O−20% $(CD_3)_2CO$ solution at 283 K, while our calculation is in either gas phase or pure water at 298 K. These calculations predict a slight upfield shift of ^{4}OH, ^{5}OH, and ^{6}OH upon deprotonation of the phosphate group as the pH increases, which is also in good agreement with the experimental results. Normally as the strength of hydrogen bonding increases, there is more proton deshielding and a larger chemical shift.

I.5. Solvation Effects. These *myo*-inositol phosphates are highly water soluble molecules. Since inositol phosphates and the inositol phosphate-containing lipids play important roles in cells, it is important to study the effects of the solvent. They are often attached as lipid headgroups and are not buried inside the protein or hydrophobic environment but are exposed to the physiological fluid. Therefore, the solvent molecules may disturb the HBN and have an effect on the preferred stable conformation. We studied the solvation effect by both implicit and explicit solvent models as discussed above. Our results show that solvent molecules can participate in the HBN by breaking weak hydrogen bonds between the vicinal hydroxyl groups and then bridging them by forming two more hydrogen bonds. But the patterns of the HBN persist regardless of the degree of deprotonation.

For Ins(2)P_1^0 and Ins(2)P_1^{1-}, the clockwise one-directional HBN is kept while even interacting with water molecules as shown in Tables 6. Compared to the isolated molecular structure in Table 1, we notice that the short hydrogen bonds are only slightly affected by the solvent molecules. The strongest hydrogen bonds of the isolated molecule are conserved as the strongest hydrogen bonds in the complexes with water molecules. The bond length change is less than 0.05 Å. The shortest hydrogen bond with a length of 1.775 Å in Ins(2)P_1^0 is changed to 1.724 Å in the complex of Ins(2)P_1^0 with water molecules, while the shortest one with a length of 1.638 Å in Ins(2)P_1^{1-} is altered to 1.687 Å.

The green dashed lines in Table 6 entries a and b indicate the distance between connected atoms that form a hydrogen bond between the vicinal hydroxyl groups in the isolated molecule state.

Therefore, the characteristic peaks (chemical shifts) in NMR, as discussed above, could remain unaffected. A similar trend is also observed in the case of Ins(2)P_1^{2-}. The HBN pattern is maintained, and the strong hydrogen bonds show little change. In Table 6 entry c, the optimized structure starting from the

Table 6. Solvation Effect on the Intra-HBNs of Ins(2)P_1 and Its Anions[a−c]

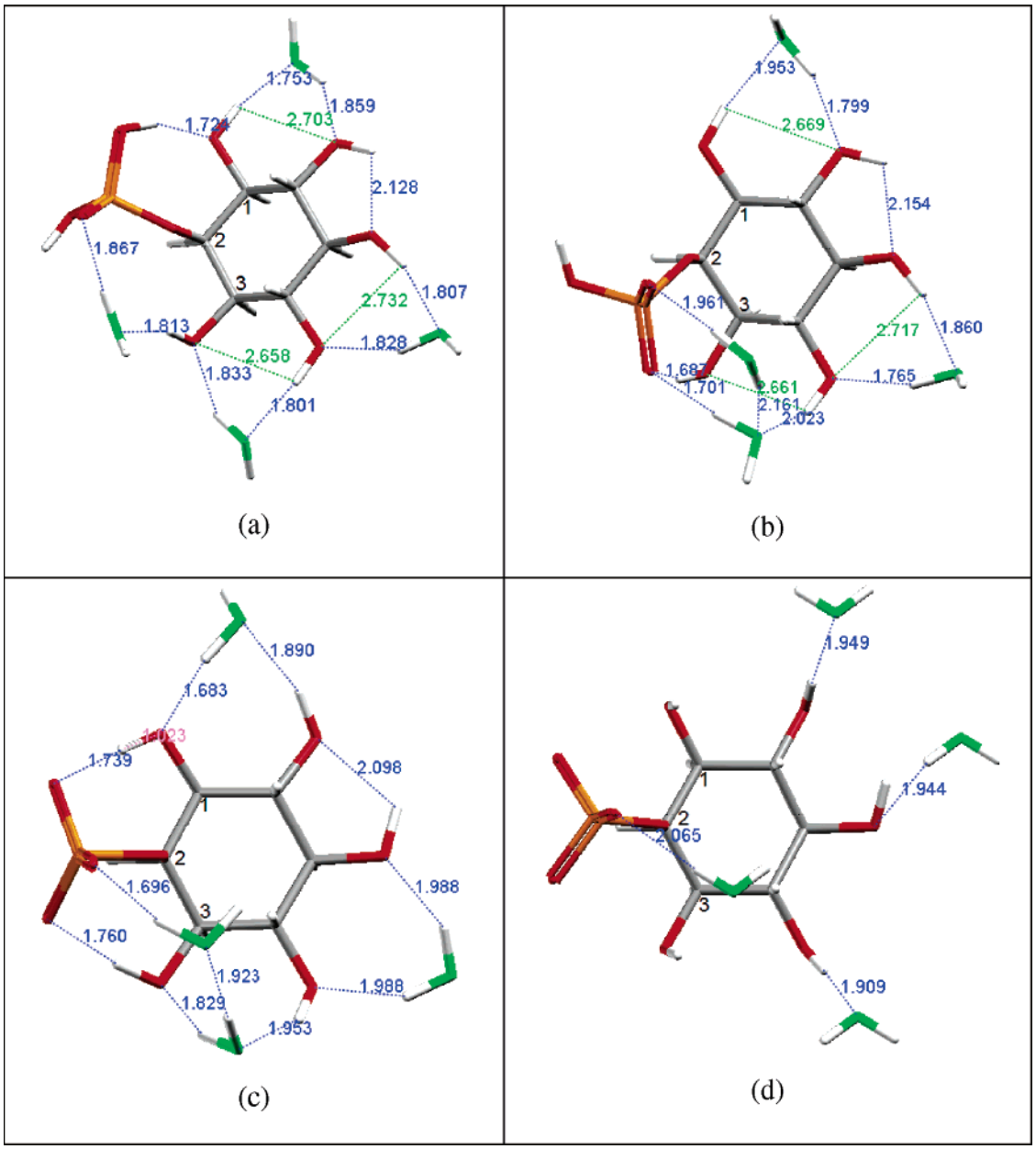

[a] Oxygen atoms in water are shown in green. [b] The green labeled numbers are for the distance between the two connected atoms. [c] (a) Optimized structure of Ins(2)P_1^0 with four water molecules. (b) Optimized structure of Ins(2)P_1^{1-} with four water molecules. (c) Optimized structure of Ins(2)P_1^{2-} with four water molecules. (d) Crystal structure of Ins(2)P_1^{2-} with four water molecules.

relaxed one in the gas phase is exactly the same as the optimized structure starting from the crystal structure in Table 6 entry d.[69] The crystal structure is different from the gas phase geometry due to the packing effect between layers. Compared to explicit solvent simulations, implicit solvent calculations actually give an accurate representation of the HBN with good agreement with experimental data. Henceforth, we will use the implicit model (PCM) for solvation effect calculations.

II. Proton Transfer. The minimized geometries of the 1a/5e and 5a/1e conformations of Ins(2)P_1^{2-} with and without proton transfer are shown in Table 7. The calculated energy and energy difference between conformations in gas phase and aqueous phase are presented in Table 8. These data provide insight into the optimum configurations of the intramolecular hydrogen bonding networks as well as the effect of the solvation on the intrinsic intramolecular proton migration. Proton transfer is an important component of the mechanism of many enzymes such that developing not only an understanding of the relevant conformations but also the energetics/thermodynamics is important.

In the 1a/5e conformation, two relatively strong hydrogen bonds between the phosphate group and the vicinal ^{1}OH and ^{3}OH hydroxyl groups result in the formation of two unidirectional (head-to-tail) networks of hydrogen bonds which take advantage of many-body nonadditive interactions known as hydrogen bond cooperativity.[28] The conformation resulting from a transfer of the ^{1}OH proton is 4.1 kcal/mol lower in energy and thus is the global minimum in the gas phase, while the conformation resulting from the transfer of the ^{3}OH proton gives a conformation that is 6.24 kcal/mol higher in energy. The HBN reduces or destroys all symmetry in the Ins(2)P_1 molecule. The two types of proton transfer end up with different H-bond

Table 7. Ins(2)P_1^{2-} Conformations before and after Proton Migration[a]

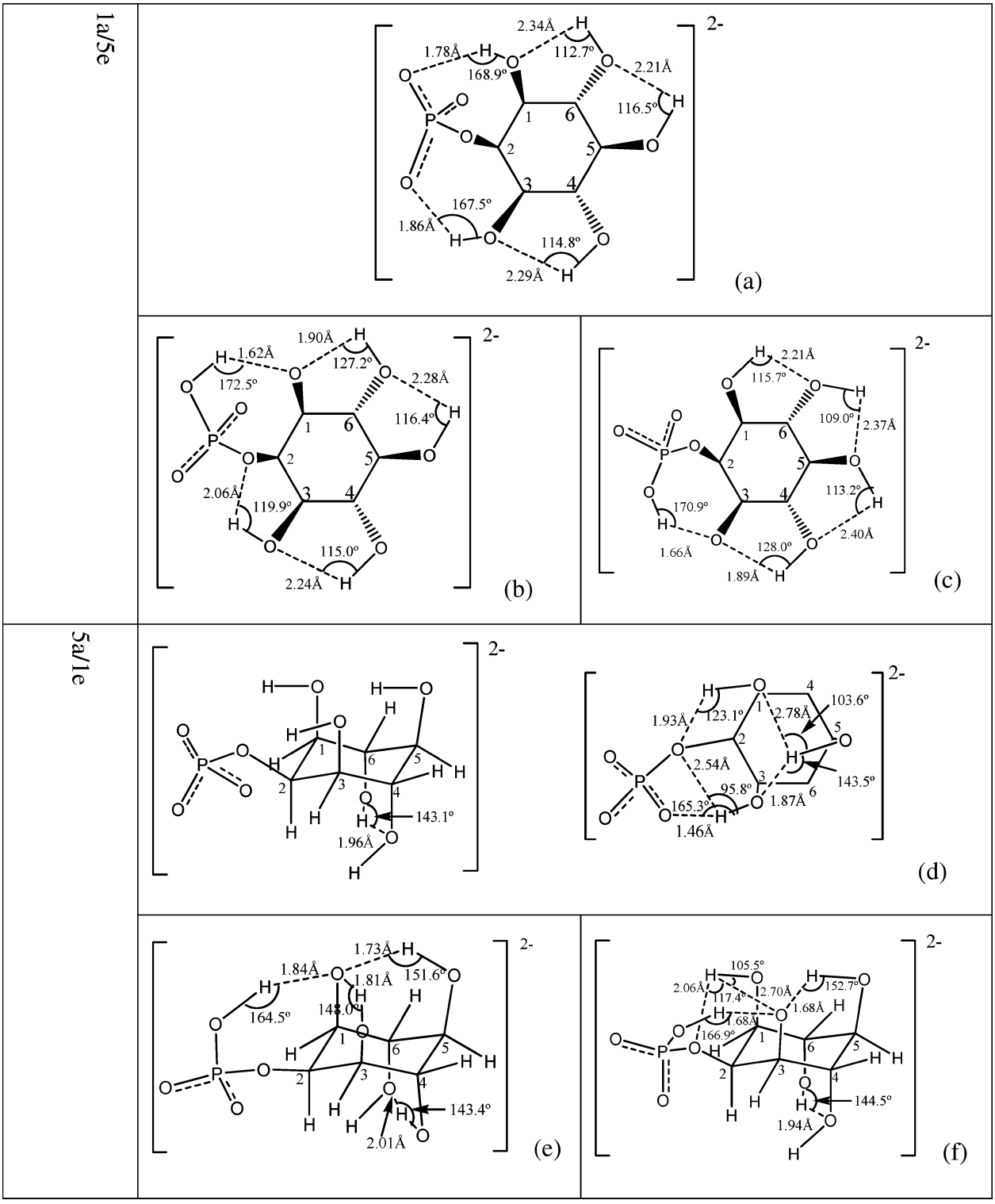

[a] (a) 1a/5e conformation without proton transfer (global minimum in water). (b) 1a/5e conformation after proton transfer from ^{1}OH group (global minimum in gas phase). (c) 1a/5e conformation after proton migration from ^{3}OH group. (d) 5a/1e conformation without proton transfer. (e) 5a/1e conformation after proton transfer from ^{1}OH group. (f) 5a/1e conformation after proton transfer from ^{3}OH group.

patterns having different energies. For both, the configurations of the hydrogen bonding network are rearranged upon the proton transfer, and both benefit from cooperativity to some extent. In fact, for the ^{3}OH proton transfer, one of the hydrogen bond networks shows a reversal of directionality. An attempt to localize the transition states of the proton transfer showed that the hydrogen bonds between the phosphate and its vicinal hydroxyl groups are Low-Barrier H-Bonds (LBHB) with an activation energy that is less than 0.5 kcal/mol or no energy barrier at all. The shared proton is delocalized between the donor and acceptor oxygen atoms. Although the exact role of LBHBs in enzyme catalysis is still debated, this type of interaction has been observed in many active sites of enzymes by NMR spectroscopy.[86,87] The experimental observation of a proton

Table 8. Energy Difference between Conformations

	without proton transfer (E_p)	^{1}OH proton transfer (E_{OH1})	^{3}OH proton transfer (E_{OH3})
1a/5e conformation	−1253.5658[a]	−1253.5723	−1253.5558
($E - E_p$)	(0.0)[b]	(−4.06)	(6.24)
	−1254.0541[c]	−1254.0453	−1254.0426
	(0.0)[d]	(5.57)	(7.25)
5a/1e conformation	−1253.5585	−1253.5667	−12553.5644
($E - E_p$)	(0.0)	(−5.16)	(−3.67)
	−1254.0421	−1254.0372	−1254.0357
	(0.0)	(3.09)	(4.02)
$E_{(1a/5e)} - E_{(5a/1e)}$	−4.56[b]	−3.51	−5.40
	−7.53[d]	−5.08	−4.33

[a] The energy in gas phase in au with zero-point energy (ZPE) correction. [b] The energy change due to proton transfer in gas phase in kcal/mol. [c] The energy in aqueous phase in au with ZPE correction. [d] The energy change due to proton transfer in aqueous phase in kcal/mol.

transfer between a phosphate group and a hydroxyl group has not been reported yet. More carefully designed experimental and theoretical research are needed to find possible mechanisms involving the LBHB between the deprotonated phosphate group and hydroxyl groups.

As shown in Table 8, solvation plays a significant role in the stabilization. In aqueous solution, the initial configuration, without proton transfer, has the lowest energy and is the global minimum of the entire system. Its energy is 5.57 and 7.25 kcal/mol lower than the corresponding conformations after proton transfer. So, in water, the Ins(2)P_1^{2-} exists primarily without proton migration. The results show good agreement with NMR experimental data.[24] Using the GIAO method we found that the protons of the hydroxyl groups vicinal to the phosphate group gave bands at 6.97 and 6.16 ppm for ^{1}OH and ^{3}OH, respectively, for only the 1a/5e conformation while experiment gave a broad signal at 6.9 ppm. Interactions between phosphate and hydroxyl groups often occur in a hydrophobic environment common to the interior of proteins and membranes where the gas phase results should give a good approximation. These results show that the proton transfer is thermodynamically favorable. The mechanism for the transfer of a proton across a membrane may indeed involve these specific kinds of interactions.

Note that, for the corresponding 5a/1e chair form after ring inversion, the hydroxyl group ^{3}OH is involved in a very short hydrogen bond (1.46 Å) and a lengthened O−H bond (1.068 Å, elongated by 0.088 Å) as shown in the middle of the last row in Table 1. Proton transfer from the ^{1}OH and ^{3}OH groups in the gas-phase stabilizes the system by 5.16 and 3.67 kcal/mol, respectively. As noted above, solvation plays a key role in the system energy. The conformations of the 5a/1e conformation after proton transfer (Table 7 entries e and f) are also unstable in water compared to the initial conformation.

Notably, the 5a/1e conformation after proton transfer has a four-center hydrogen bond involving the oxyanion. The conformation after the ^{1}OH proton transfer has relatively strong hydrogen bonds with lengths of 1.73 Å, 1.81 Å, and 1.84 Å at the four-center hydrogen bond. This four-center hydrogen bond network stabilizes the system in the gas phase and lowers the energy below that of the 1a/5e conformation. This phenomenon was not found in Ins(2)P_1^0 and Ins(2)P_1^{-1} in our previous work. The conformation formed by ^{3}OH proton transfer is less stable due to a very weak hydrogen bond (2.7 Å) in the four-center hydrogen bond network. Actually, the four-centered structure is weakened or almost broken up by a strong hydrogen bond between the ^{3}OH hydrogen and the phosphate oxygen. Proton transfer is crucial to energy transfer (ET) reactions, where phosphate groups are often involved. This exceptionally stable hydrogen bond prototype and low barrier proton transfer via a strong hydrogen bond between the phosphate group and hydroxyl group could help understand those ET mechanisms at the atomic level.

Natural bond orbital (NBO) theory[88−91] has been used to determine the relative significance of local orbital interactions in the context of a donor−acceptor model and to demonstrate and quantify electronic interactions such as those involved in hyperconjugation, the anomeric effect, and charge transfer in hydrogen bonding. An NBO analysis is helpful in understanding intramolecular non-Lewis delocalizations in terms of localized one- and two-center orbitals. In this manner, H-bond formation can be viewed as a result of charge transfer from a lone pair or bonding orbitals of the acceptor into antibonding orbitals of the H-bond donor. The amount of energy stabilization, $E^{(2)}$ [92] due to interaction can be associated with significant charge-transfer interactions. NBO population analysis calculations were performed on the optimized structures to approximate and compare the relative contributions to the stabilization energy arising from charge transfer for any O−H···O donor−acceptor complex (H-bonded complexes) shown in the calculated geometries. The three lone pairs on the oxyanion ^{7}O form strong donor−acceptor interactions with the σ^* antibonding orbitals of ^{9}O−^{21}H, ^{11}O−^{23}H, and ^{28}O−^{19}H giving a stabilization energy, $E^{(2)}$, of 21.88, 29.57, and 17.27 kcal/mol, respectively. In the gas phase, this conformation is 5.16 kcal/mol lower than the 1a/5e conformation. The chemical shift δ values are 6.31, 6.96, and 6.96 ppm for ^{21}H, ^{23}H, and ^{19}H, respectively.

III. Transition States. The structures of the transition state (TS) are the key to understanding the chair-to-chair inversion process. These states have one and only one imaginary vibrational frequency. A careful TS/energy analysis allows one to eliminate those conformations that are not chemically significant, i.e., those which are either kinetically inaccessible or thermodynamically unpopulated. For complex systems, this can considerably reduce the number of options that must be considered.

In all the transition states, the ring is twisted and part of the hydrogen-bonding network is conserved. Each transition state for Ins(2)P_1^0, Ins(2)P_1^{1-}, and Ins(2)P_1^{2-} have four hydrogen bonds remaining and shorter O···H bond lengths compared to their corresponding 5a/1e or 1a/5e conformations. The dipole moment of the transition states are closer to that of 5a/1e conformations. Overall, the transition states are more 5a/1e-like. The two hydrogen bonds formed between the oxygen atoms of the phosphate group and its vicinal hydroxyl groups survive the inversion and become stronger. The data also indicate that as the degree of deprotonation increases, the surviving hydrogen

(86) Frey, P. A. *Magn. Res. Chem.* **2001**, *39*, S190−S198.
(87) Cleland, W. W.; Kreevoy, M. M. *Science* **1994**, *264*, 1887−1890.
(88) Carpenter, J. E.; Weinhold, F. *THEOCHEM* **1988**, *169*, 41−62.
(89) Foster, J. P.; Weinhold, F. *J. Am. Chem. Soc.* **1980**, *102*, 7211−7218.
(90) Reed, A. E.; Weinhold, F. *J. Chem. Phys.* **1983**, *78*, 4066−4073.
(91) Reed, A. E.; Weinhold, F. *Chem. Rev.* **1988**, *88*, 899−926.
(92) Weinhold, F. In *Encyclopedia of computational chemistry*; Schleyer, P. v. R., Allinger, N. L., Clark, T., Gasteiger, J., Kollman, P. A., Schaefer, H. F. I., Schreiner, P. R., Eds.; John Wiley & Sons: Chichester, U.K., 1998; Vol. 3, p 1792.

Table 9. pK_a Values of Ins(2)P_1

		$Ins(2)P_1^0 \rightarrow Ins(2)P_1^{1-}$			$Ins(2)P_1^{1-} \rightarrow Ins(2)P_1^{2-}$		
		pK_aA	pK_aB	pK_a1	pK_aC	pK_aD	pK_a2
1a/5e	HF/6-31+G(d)	1.89	1.32	1.22	4.72	5.30	5.85
(>93%)	B3LYP/6-31+G(d)	1.04	0.46	0.36	3.50	4.07	4.17
5a/1e	HF/6-31+G(d)	2.08	2.92	2.02	5.25	4.40	5.31
(<7%)	B3LYP/6-31+G(d)	1.18	0.44	0.37	6.28	7.01	7.09

[a] Note: A refers the hydrogen atom on the phosphate group which contributes to the intra-HBN. B refers the hydrogen atom on phosphate group which is not a part of the intra-HBN. Once A and B dissociates, the remaining hydrogen on the phosphate group is C or D, respectively.

bonds strengthen. The transition state for $Ins(2)P_1^0$ has a flatter ring than those for the charged species. The deprotonated species $Ins(2)P_1^{1-}$ and $Ins(2)P_1^{2-}$ have a more puckered ring due to the larger electrostatic attraction between the charged phosphate group and other hydroxyl groups.

The activation energy for the ring-flip can tell us how easily the ring inverts. In the gas phase, the activation energy for the global minimum (1a/5e conformation) is 18.53 kcal/mol for neutral inositol monophosphate $Ins(2)P_1^0$, 10.51 kcal/mol for $Ins(2)P_1^{1-}$, and 6.37 kcal/mol for $Ins(2)P_1^{2-}$. It is obvious that the more charged species are more prone to ring inversion in vacuo. When the solvation effect is included, the activation energy is much less sensitive to the charge and is 18.16, 15.62, and 12.48 kcal/mol respectively (Table 5). For the same basis sets, the B3LYP method gives lower activation energies than the HF method. The thermal ring inversion will not occur in either phase based on predicted high activation energies.

For the transition state of $Ins(2)P_1^0$, the dipole moment is higher than either of its corresponding chair forms, while, for $Ins(2)P_1^{1-}$, the transition state has a dipole moment between those of its two chair forms. But, for $Ins(2)P_1^{2-}$, no such trend is observed. The dipole moments for its chair forms and transition state are relatively close to each other due to full deprotonation. The solvent induced components of the dipole moment are 20% for the HF calculations and 28% for the DFT calculations regardless of the size of the basis sets.

For all conformations, the solvent affects are larger for the charged molecules, increasing from $Ins(2)P_1^0$ to $Ins(2)P_1^{1-}$ and to $Ins(2)P_1^{2-}$. For example, the Gibbs free energies of solvation for the 1a/5e conformations are −27.41 kcal/mol, −64.44 kcal/mol, and −181.95 kcal/mol, respectively. For the neutral species, the solvation effect for the transition state is larger than those for their chair forms, whereas, for the charged species, the solvation effect for the transition state lies between those for the two chair forms. The interaction between solvent and solute increases the activation energy, and thus the ring inversion in water is even more unfavorable than in the gas phase, as shown in Table 5.

IV. Absolute pK_a Values. It is well-known that proton-transfer reactions are common in chemical and biological reactions Thus the evaluation of pK_a values is important for understanding the mechanisms of enzymes.

Predicting the pK_a values becomes more complicated when the acid contains more than one possible ionized proton. The concept of microconstants is used here to understand and calculate accurate pK_a values. The possible equilibria for the case of $Ins(2)P_1$ are shown in Figure 4. There are four microscopic equilibrium constants (k_A, k_B, k_C, and k_D) and two overall (observable) macroscopic equilibrium constants (K_1 and K_2). The microscopic constants can be predicted directly from

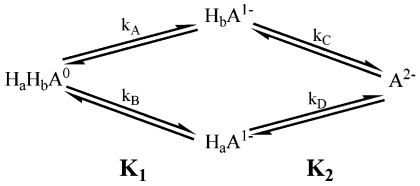

$$K_1 = k_A + k_B$$

$$\frac{1}{K_2} = \frac{1}{k_C} + \frac{1}{k_D}$$

Figure 4. The dissociation equilibria for diprotic acid Ins(2)P_1, (A = Ins-(2)P_1).

the results of theoretical calculations. By the following relationships between these microscopic and macroscopic constants,[93] the macroscopic constants can be easily calculated.

All protonation states are included in calculating the pK_a values. Two possibilities are considered, i.e., one for each of the two hydrogen atoms on the phosphate group in the neutral form of $Ins(2)P_1^0$. The hydrogen atom participating in the intra-HBN is labeled as H_a, while the other which is not a part of the HBN is labeled as H_b. Micro equilibrium constant k_A controls the reaction when H_a protonates from the molecule. A similar notation applies for H_b.

Even though the population of 5a/1e is very small (<7.0%), the theoretical pK_a values are estimated as well and given in Table 9. The population analysis is based on the Boltzmann distribution law. The predicted pK_a values for the 1a/5e conformation, which should be the naturally dominant one in water, are 1.22 and 5.85 as calculated at the HF/6-31+G(d) level. The second pK_a agrees with experimental data perfectly. The Spiess group determined pK_a2 equal to 5.83 in 0.1 M tetrabutylammonium bromide ($n$$Bu_4NBr$) as supporting electrolyte and 5.54 and 5.56 at 25 °C, respectively, in 0.1 M KCl and 0.1 M NaCl.[94] The B3LYP/6-31+G(d) method produces poorer agreement with the experimental data with numbers of 0.36 and 4.17 for the 1a/5e conformation, but still within 1.5 pK_a units. As expected, the hydrogen atom which is part of the HBN is less acidic compared to that which is not hydrogen bonded, since it gives larger microconstant pK_a values in both conformations. As a result, for accurate pK_a prediction, the effects of hydrogen bonding have to be considered.

Conclusions

In this paper, we present a theoretical ab initio approach to investigate an intramolecular hydrogen bonding network. Properties of conformational isomers including size, shape, and energy, as well as chemical reactivity and biological properties, including binding interactions with proteins and chelating ability

(93) Perrin, D. D.; Dempsey, B.; Serjeant, E. P. *pK_a Prediction for Organic Acids and Bases*; Chapman and Hall: London, 1981.
(94) Mernissiarifi, K.; Schmitt, L.; Schlewer, G.; Spiess, B. *Anal. Chem.* **1995**, *67*, 2567−2574.

with metal ions, can be significantly different. The conformational flexibility of biomolecules, such as inositol phosphates, has a major impact on binding interactions with enzymes and receptors and thus on biological properties due to the very specific interactions essential for biological activity. A detailed understanding of the intramolecular hydrogen bonding interactions, solvent interactions, and accessible conformations is essential for a complete understanding of enzyme−substrate and ligand−receptor binding interactions in the cellular milieu. Our main purpose is to contribute to the understanding of the structural and electronic properties of the model system, *myo*-inositol 2-monophosphate Ins(2)P_1^0, and the anions Ins(2)P_1^{1-} and Ins(2)P_1^{2-}. A novel intramolecular four-center hydrogen bond was found to stabilize the system. For the charged species, the intramolecular proton transfer through a hydrogen bond between the phosphate and hydroxyl group can occur with a low barrier.

The thermally accessible minima of these compounds were investigated using conformational search techniques. All these forms take the 1a/5e structure as the stable global conformation in both the gas phase and aqueous phase. The corresponding chair form after ring inversion to the 5a/1e structure has a comparatively higher energy in all cases. All of the conformations including the transition states are stabilized by an intramolecular hydrogen-bonding network with hydrogen bond lengths ranging from 1.46 to 2.51 Å. These hydrogen bonds are formed between the phosphate group and its vicinal hydroxyl groups as well as between various hydroxyl groups. In the 1a/5e conformations of Ins(2)P_1^0 and Ins(2)P_1^{1-}, a cyclic hydrogen bonding pattern helps to stabilize the structures. This pattern was broken up in the 1a/5e conformation of Ins(2)P_1^{2-} in order to form two hydrogen bonds between the phosphate group and its two vicinal hydroxyl groups. In the 5a/1e conformations of the anions, some oxygen atoms are involved in more than one hydrogen bond. The pairing and orientation of the hydrogen bonds depend on the charge and conformation of the molecule. Four of the hydrogen bonds survive in the transition structures, which resemble the 5a/1e conformations. These data suggest that the facile inversion of higher phosphroylated derivatives, such as the pentakis- and hexakisinositol phosphates, to the 5a/1e form could be partially due to the lack of a stabilizing HBN in the 1a/5e form.

Solvation effects result in an increase in the activation energy. The significance of the solvent induced component of the dipole moment is about 20% for the HF calculations and 25∼30% for the B3LYP calculations. The more highly charged species have a lower activation energy and are more prone to ring inversion in either phase. Both in-vacuo and water, the ring inversion for the chair to chair inversion is prohibited by a high-energy of activation; for Ins(2)P_1^0, Ins(2)P_1^{1-} and Ins(2)P_1^{2-} the activation energies are 18.16, 15.62, and 12.48 kcal/mol respectively.

For the naturally dominant species, the 1a/5e conformation, the predicted pK_a values, 1.22 and 5.85, are consistent with experimental data. The hydrogen atom which is part of the HBN is less acidic than the one not hydrogen bonded. The agreement of the predicted pK_a values and NMR spectra with the experimental results lends strong support to the observations that most of the intramolecular hydrogen bonding network remains intact after the inclusion of solvent effects.

Phosphoryl inositol-containing molecules play various key roles in biological systems. How such complex systems respond to these molecules depend highly on their dominant conformations and the flexibility for conformation change. This work represents an initial step to theoretically characterize the dominant conformations and the forces that select them. These results were validated by achieving good agreement between the theoretical and experimental values for the pK_a and NMR spectra. This report of proton transfer between a deprotonated phosphate group and a vicinal hydroxyl group will add to our understanding of energy transfer mechanisms in biological systems.

This work highlights the fact that to perform accurate simulations on biological systems, nonbonded interactions, in particular hydrogen bonding interactions, must be treated precisely due to their profound effects on molecular properties. The ab initio results presented here for these particular systems should provide excellent model systems for developing new or improved force fields that can treat the nonbonded and bonded interactions in a balanced manner.

Acknowledgment. The authors are grateful to Professor Bernard Spiess for his helpful discussions about the experimental data. Thanks are also due the National Science Foundation for a generous grant of teragrid supercomputing resources (Grant Number CHE040041N).

Supporting Information Available: Tables of molecular coordinates, molecular dipole moments, hydrogen bond lengths and angles, the bond length changes of the hydroxyl groups due to the formation of hydrogen bonds, and the chemical shifts for the optimized structures. This material is available free of charge via the Internet at http://pubs.acs.org.

JA053371U